

# OIL & CHEMICAL POLLUTION

Completes the  
1989 subscription

*Oil & Chemical Pollution* 5 (1989) 411-449

## A Coastal Zone Oil Spill Model: Development and Sensitivity Studies

Mark Reed,<sup>a</sup> Erich Gundlach<sup>b</sup>

<sup>a</sup>Applied Science Associates, Inc., <sup>b</sup>E-Tech, Inc., 70, Dean Knauss Drive, Narragansett, Rhode Island 02882, USA

&

Timothy Kana

Coastal Science and Engineering, Inc., PO Box 8056, Columbia, South Carolina 29202, USA

(Received 27 October 1988; accepted 6 November 1988)

### ABSTRACT

*Oil spill trajectory and fates models typically follow a surface slick until it contacts a coastline, at which time the simulation ceases. The coastal zone oil spill (COZOIL) model described here is designed to simulate oil spill fates both before and after a coastal contact. Multiple discrete batches of oil (spillets) are used to represent the surface slick. Spillets are circular while offshore but become elliptical upon contact with the shoreline. Onshore-offshore foreshortening is governed by a balance between wind stress and gravity spreading forces, and results in alongshore spreading of the spillet. Evaporated hydrocarbons are accumulated from all sources during the simulation, with no spatial representation. Entrained oil offshore is represented by discrete particles which may be advected by the local currents. Inside the surf zone, entrained oil takes on a continuous representation, discretized within individual alongshore grid cells. Transport in the surf zone is governed by a classical radiation stress formulation. Incorporation of water into surface oil (emulsification) is simulated offshore. De-emulsification (de-watering) is allowed to occur for oil which is on the foreshore or backshore. Oil coming ashore may be deposited on the foreshore or the backshore, or carried into coastal indentations (lagoons, ponds, or fjords). Each of the seven shoreline*

411

*Oil & Chemical Pollution* 0269-8579/89/\$03.50 © 1989 Elsevier Science Publishers England. Printed in Ireland.

types represented in COZOIL is characterized by a unique set of parameters, including grain size, porosity, and a maximum oil thickness which the foreshore can retain. Oil on the foreshore penetrates into the underlying sediments at a rate dependent on sediment grain size and oil viscosity. Oil may also be carried into the beach groundwater system by wave overwash. Reflotation of surface oil occurs during rising tides. The model is inherently deterministic with respect to results of any single simulation. Stochastic oil distribution estimates are produced by combining the results of multiple simulations, each of which may be driven by a separate weather scenario.

## 1 INTRODUCTION

A longstanding problem in oil spill modelling has been the realistic simulation of spill behavior after contact with a shoreline. Two statistical regression models have been developed previously to attempt to correlate length of coastline affected with oil spill size (Ford, 1985; Seip *et al.*, 1986). By converting to log-log space, Ford (1985) was able to explain about 65% of the total variance in coastline affected using latitude and volume as the independent variables. The per cent explained would presumably be considerably reduced in linear regression. Seip *et al.* (1986) found no correlation between shore length damaged and the amount of oil spilled. Results of these efforts show the statistical approach to be relatively unsatisfactory for determining the probable extent of the shoreline impacts problem.

The coastal zone oil spill (COZOIL) model described here was designed to include explicit representations of the active processes affecting a spill. Multiple discrete batches of oil, or spilletts, are used to represent the surface slick. Spilletts are circular while offshore but become elliptical upon contact with the shoreline. Onshore-offshore foreshortening is governed by a balance between wind stress and gravity spreading forces, and results in alongshore spreading of the spillet. Evaporated hydrocarbons are given no spatial representation, but are simply accumulated from all sources during the simulation. Entrained oil offshore is represented by discrete particles which are advected by the local currents. Inside the surf zone, entrained oil takes on a continuous representation, discretized by alongshore grid cell. Transport in the surf zone is governed by a classical radiation stress formulation. Incorporation of water into surface oil (emulsification) is simulated offshore. De-emulsification (de-watering) is allowed to occur for oil which is on the foreshore or backshore.

Oil coming ashore may be deposited on the foreshore or the

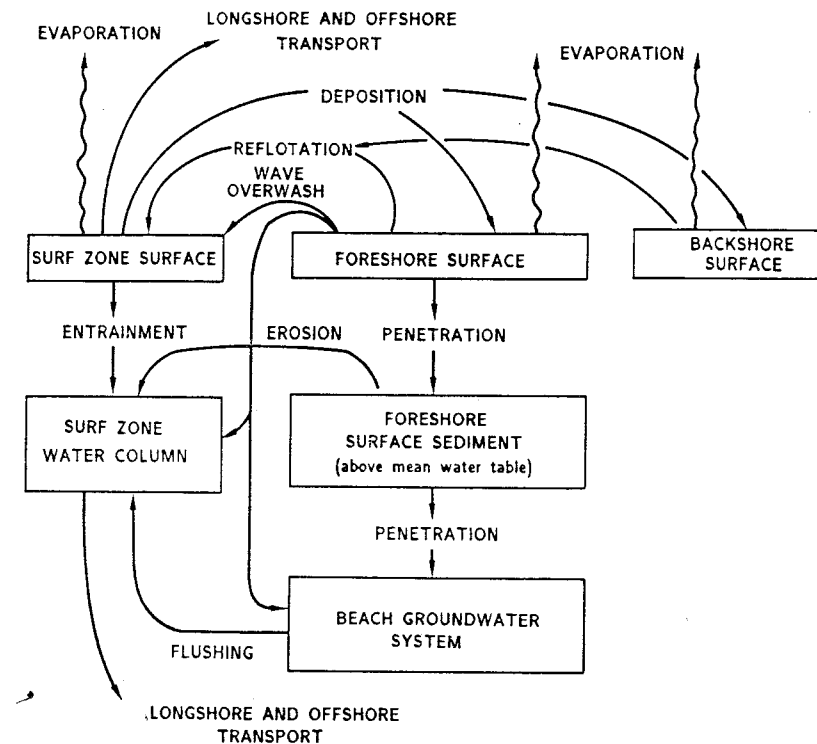


Fig. 1. COZOIL mass-transfer pathways in the coastal zone.

backshore, or carried into coastal lagoons, ponds, or fjords. Oil on the foreshore penetrates into the underlying sediments at a rate dependent on sediment grain size and oil viscosity. Oil may also be carried into the beach groundwater system by wave overwash. Reflotation of surface oil occurs during rising tides. These mass transfer pathways are shown schematically in Fig. 1.

## 2 COZOIL MODEL SYSTEM OVERVIEW

The COZOIL model can be conceptually divided into a set of initialization processes, followed by computational and output routines (Fig. 2). During initialization, the spill scenario is established, including specification of oil type, spill size and duration, simulation duration and study area topography and geology.

The program leads the user through initialization via a series of queries. The most complex portion of the initialization process is the

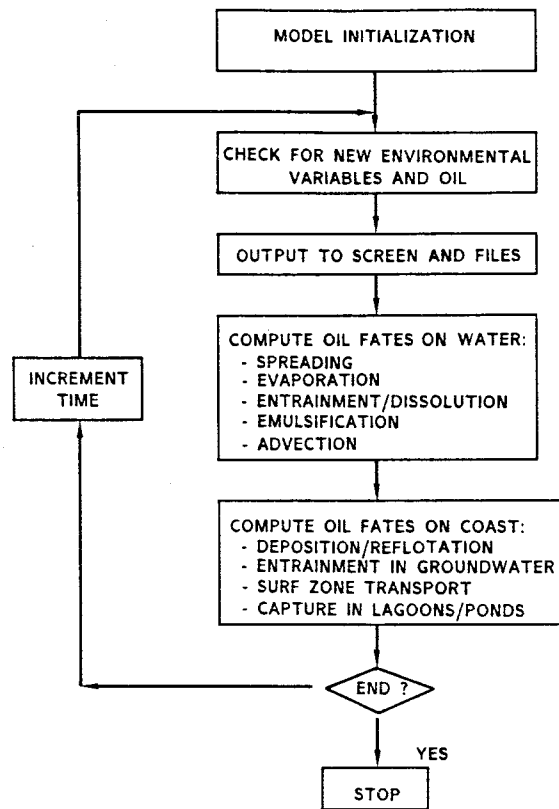


Fig. 2. COZOIL model system schematic.

establishment of the geophysical environment within which the simulation will take place. The second important part of the model initialization process centers on the specification of the environmental data used to drive the simulation. First the user must either direct the model to access an existing wind data set, or input a new time series. The model then requests the name of an existing tidal current data set, or sufficient data to create one. A wind-driven current data set is then created by the model from the wind record, if the user does not specify an existing data set. Finally, the model either computes waves from the wind record, or accesses a wave time series from an external file.

Model output is controlled by the program itself; the user controls only the time interval between outputs to the screen and to data storage files. Outputs at the end of each time interval include boiling point cut information by surface spillet and coastal reach, an overall mass balance, and line plots showing the location of surface spilletts and the alongshore

distribution of hydrocarbons. COZOIL also tells the user when new environmental data is being read into the model, and shows the results of ensuing wave height and angle computations. If the user selects the abbreviated output option, much of this secondary information is suppressed.

### 3 PHYSICAL ENVIRONMENTAL CONCEPTS AND ALGORITHMS

In this section we discuss the physical concepts embodied in the model, including the grid system, the specification of coastal reaches and bathymetry, as well as wind, wave, and current data inputs.

The COZOIL model runs on a rectangular grid system oriented such that the first subscript (I) runs from west to east, and the second (J) from south to north (Fig. 3). The dimensions of a single grid cell are a function of the specified size of the study area and the dimension of the governing arrays in the model. In our example of Fig. 3, the study area is about  $20 \times 70$  km. If it is compiled with a  $10 \times 10$  grid system, grid size for this case will be 2000 m onshore-offshore (east-west) and 7000 m alongshore (north-south). At this study area size and array size, no reaches shorter than 7000 m north-south (or 2000 m east-west) will be resolved. To increase the resolution (i.e. achieve a smaller grid cell size), one can either decrease the study area size or re-compile the model with larger arrays.

There are eight types of coastal reaches defined in the present version of the COZOIL model:

- (1) smooth rocky shore or sea-wall
- (2) cobble beach
- (3) eroding peat scarps
- (4) sand beach
- (5) gravel beach
- (6) tidal (mud) flat
- (7) marsh
- (8) coastal pond, lagoon, or fjord

For each of reach types (1)-(7), there are eight parameters required by the model:

- (1) reach length (m)
- (2) backshore width (m)
- (3) foreshore width (m)
- (4) offshore distance (m)

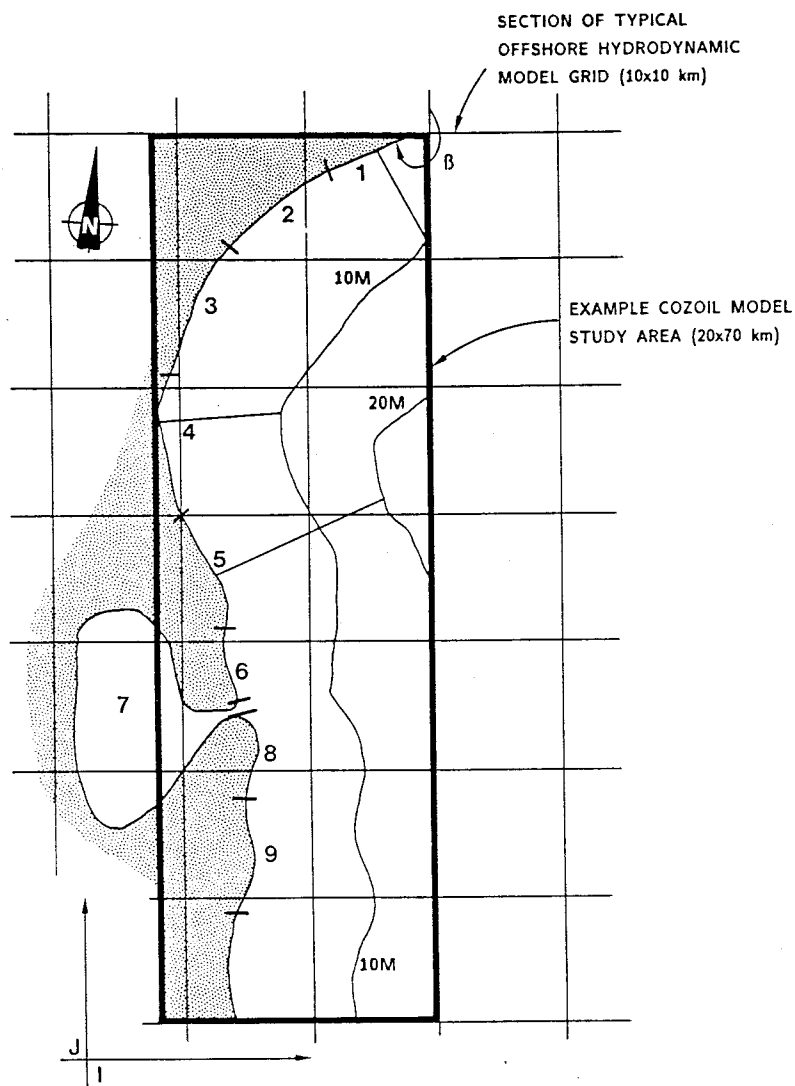


Fig. 3. Example COZOIL model study area, showing a typical offshore hydrodynamic model grid, bathymetry, and division of shoreline into reaches.

- (5) backshore slope (rise/run)
- (6) foreshore slope (rise/run)
- (7) offshore depth (m)
- (8) reach orientation (degrees)

The identification of parameters (2)–(7) is given in Fig. 4. The fore-

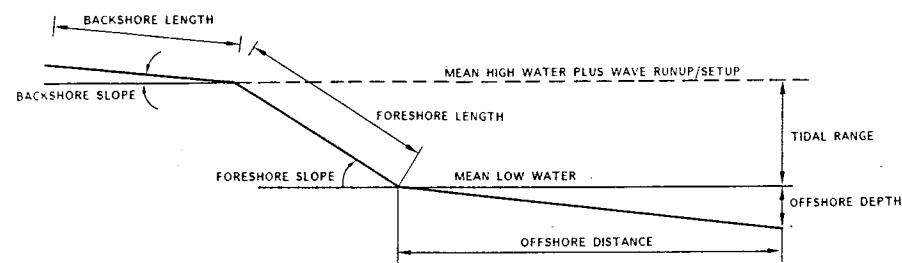


Fig. 4. Definition of input parameters for coastal reaches (except coastal inlets).

shore is defined to extend from the mean low-water line to the berm. The backshore extends from the berm to the dunes, cliffs, or first permanent onshore vegetation. Parameter (8), reach orientation, is measured in degrees clockwise from true north, standing at the beginning of the reach with water on the left. Thus in our example case, Fig. 3, reach no. 1 is at the top of the figure, and has an orientation  $\beta$  of about  $240^\circ$ . The offshore distance (parameter (4)) and the offshore depth (parameter (7)) are used to determine the mean bathymetric slope. The model uses linear interpolation among the offshore depths specified for all reaches to create a discretized representation of the bathymetry.

For reach type (8), the model requests four parameters:

- (1) pond surface area ( $m^2$ )
- (2) breachway (entrance) width (m)
- (3) breachway (entrance) depth (m)
- (4) tidal range inside the pond (m)

Flow into and out of coastal ponds and lagoons is computed by simple conservation of mass principles, assuming uniform velocities over the entrance cross section, and neglecting phase lags inside and outside the pond.

### 3.1 Wind

The model assumes a uniform wind field over the study area. Since coastal zone study areas are generally expected to be small (e.g. 100 km alongshore and 1–20 km offshore), spatial variability in the wind field will in general be difficult to resolve from commonly available data.

The user may manually input a wind time series, or direct the model to access a prepared data set. Wind data sets from nearby land stations are appropriate for input to COZOIL. Thus for most applications there will be an abundance of historical data for stochastic simulations. The

model is also capable of accepting a matrix of first-order Markov transition probabilities from which to compute stochastic oil spill scenarios.

### 3.2 Waves

The user can direct the model to compute waves from the wind record, or to read in a wave time series from a prepared file. In either case, the inputs to the computational model are wave height (m), wave period (s), and direction of propagation. These values are assumed by the model to apply at the offshore (open) boundaries.

If the user elects to compute waves from the wind record, the model uses the shallow water, wave forecasting equations recommended by the US Army Corps of Engineers Shore Protection Manual (CERC, 1984):

$$\frac{gH}{U^2} = 0.283 \tanh \left[ 0.530 \left( \frac{gd}{U^2} \right)^{3/4} \right] \tanh \left\{ \frac{0.00565 \left( \frac{gF}{U^2} \right)^{3/4}}{\tanh \left[ 0.530 \left( \frac{gd}{U^2} \right)^{3/4} \right]} \right\} \quad (1)$$

$$\frac{gT}{U} = 7.54 \tanh \left[ 0.883 \left( \frac{gd}{U^2} \right)^{3/8} \right] \tanh \left\{ \frac{0.00379 \left( \frac{gF}{U^2} \right)^{1/3}}{\tanh \left[ 0.833 \left( \frac{gd}{U^2} \right)^{3/8} \right]} \right\} \quad (2)$$

$$\frac{gI}{U} = 5.37 \times 10^2 \left( \frac{gT}{U} \right)^{7/3} \quad (3)$$

Refraction, diffraction, wave height and phase transformations are computed using a modified version of the CERC linear wave propagation model RCPWAVE (Ebersole *et al.*, 1986). The governing equations are (Berkhoff, 1972):

$$\frac{1}{a} \left\{ \frac{\partial^2 a}{\partial x^2} + \frac{\partial^2 a}{\partial y^2} + \frac{1}{cc_g} [\nabla a \cdot \nabla (cc_g)] \right\} + k^2 - |\nabla s|^2 = 0 \quad (4)$$

$$\nabla \cdot (a^2 cc_g \nabla s) = 0 \quad (5)$$

where the symbol  $\nabla$  denotes the horizontal gradient operator.

Together, these equations describe the combined refraction and diffraction process. The governing equations are solved using a finite

difference operator. Model input includes values of the deep-water wave height  $H_o$ , direction  $\theta_o$ , and period  $T$  of waves to be simulated. It also includes specification of the bottom bathymetry throughout the grid. The wave number, which is related to the wave period and the local water depth through the dispersion relation, is computed at every cell. Wave number is used as an initial guess for the magnitude of the wave phase function gradient. The wave celerity  $c$  and the group velocity  $c_g$  are functions of the wave period and wave number, and can therefore be calculated at each cell.

### 3.3 Wave transformation inside the surf zone

Waves approaching the very nearshore zone tend to steepen and eventually break because of decreasing water depths. Shoreward of this breaking point dissipative energy losses due to turbulence strongly influence the wave height. Linear theory allows neither for prediction of the breaker location nor for wave transformation across the surf zone. RCPWAVE uses the wave-breaking criterion of Weggel (1972):

$$H_b = \frac{bh_b}{1 + \frac{ba}{gT^2}} \quad (6)$$

where  $a = 43.75[1 - e^{(-19m)}]$ ,  $b = 1.56/[1 + e^{(-19.5m)}]$ ,  $m$  = beach slope.

Once the incipient breaking point is defined, the transformation of breaking waves across the surf zone is computed using the hydraulic jump energy loss to approximate losses across the entire surf zone (Dally *et al.*, 1984):

$$\frac{\partial(H^2 c_g)}{\partial x} = \frac{-\kappa}{h} [H^2 c_g - (\gamma^2 h^2 c_g)_s] + D \quad (7)$$

where  $\kappa$  = rate of energy dissipation coefficient (set equal to 0.2 in RCPWAVE),  $(\gamma^2 h^2 c_g)_s$  = stable level of energy flux that the transformation process seeks to attain,  $h$  = local water depth,  $H_s$  = stable wave height,  $\gamma$  = proportionality coefficient (set equal to 0.4 in RCPWAVE).

For computation of wave phase transformations within the surf zone, diffraction effects are assumed to be negligible. Therefore the wave number  $\kappa$  is assumed to accurately represent the magnitude of the wave phase function gradient. The linear wave theory assumption that the waves are irrotational also will be assumed to remain valid inside the surf

zone. Consequently, wave angles inside the surf zone are computed in the same manner as used outside the surf zone.

Both laboratory and field data were used to verify RCPWAVE. The ability of RCPWAVE to simulate wave transformation outside the surf zone was checked using data collected during a laboratory experiment conducted by Berkhoff *et al.* (1982) and using prototype data obtained during a field experiment at the CERC Field Research Facility (FRF) in Duck, North Carolina. Only laboratory data were used to verify the surf zone wave transformation part of the model. These data were collected during one-dimensional flume tests performed by Horikawa & Kuo (1966) and Izumiya (1984). Both experiments considered only breaking of monochromatic, plane waves. The former experiment investigated wave transformation on a plane beach only; the latter involved tests using plane, stepped, and barred beaches. These comparisons are discussed in detail in the source document (Ebersole *et al.*, 1986).

### 3.4 Wave Run-up and Set-up

COZOIL also requires a procedure for computing wave run-up. The vertical height above the stillwater level to which incident waves will run up a beach face depends on the shape, roughness, and permeability of the beach, as well as characteristics of the wave. A comprehensive theoretical description of this process is not available due to the large number of variables involved (CERC, 1984). In addition, most laboratory tests have been performed for smooth, impermeable slopes.

Based on the graphical procedures outlined in CERC (1984), the following approximate curve fit has been obtained:

$$R = 1.5H_o \exp(-295H_o/gT^2) \quad (8)$$

in which  $R$  = run-up distance (m),  $H_o$  = deep-water wave height (m),  $T$  = wave period (s),  $g$  = gravitational acceleration ( $m/s^2$ ).

COZOIL also incorporates a wave set-up computation based on radiation stress concepts (CERC, 1984). The net wave set-up,  $S_n$ , at the coast is the wave set-up minus the set-down:

$$S_n = 0.15h_b - (g^{1/2}H_o^2T/64\pi h_b^{3/2}) \quad (9a)$$

The depth of water at the breaker point is computed from

$$h_b = H_o/(b - (aH_o/gT^2)) \quad (9b)$$

where the coefficients  $a$  and  $b$  are as given for equation (6).

### 3.5 Currents

COZOIL uses tidal, wind-driven, and wave-induced currents to perform transport calculations. With the exception of the wave-induced currents used inside the surf zone, these data can be input directly by the user or accessed from external files. Wave-induced currents are computed inside the model as the simulation proceeds.

To compute tidal currents, the model requests two parameters from the user: tidal period and maximum tidal current amplitude. The model assumes that tidal currents are parallel to the coast (a reasonable assumption nearshore) and proceeds to compute the mean longshore direction from the input reach information. The tidal currents are then simulated as:

$$V_T = V_{\max} \sin(\omega t + \phi) \quad (10)$$

where  $V_{\max}$  = maximum tidal current amplitude,  $\omega = 2\pi/T$  (per h),  $T$  = tidal period (h),  $t$  = time (h),  $\phi$  = user input tidal phase lag at simulation start.

COZOIL incorporates a simple model (Reed, 1980) to provide an estimate of the wind-driven currents in the study area. This model incorporates the following assumptions:

- uniform currents over an upper mixed layer of depth  $H$ ,
- no flow in the vertical, and
- no surface set-up

This model is not particularly good for use near shorelines since it ignores the surface slope terms and is, therefore, less than ideal for inclusion in COZOIL. However, the wind-driven flows are not applied inside the surf zone, and are therefore most relevant with regard to transport of subsurface entrained oil offshore. Since this transport has little effect on the ultimate disposition of oil along the coastline, further improvements in this aspect of COZOIL are given relatively low priority.

The governing equations for the slab flow model are:

$$\frac{du}{dt} = fu + \frac{\tau_{xs}}{\rho_w H} - \frac{\tau_{xH}}{\rho_w H} \quad (11a)$$

$$\frac{dv}{dt} = fv + \frac{\tau_{ys}}{\rho_w H} - \frac{\tau_{yH}}{\rho_w H} \quad (11b)$$

which have the solution:

$$u(t) = \exp(-R_H t/H) [\cos(ft)(U_o - U_\infty) + \sin(ft)(V_o - V_\infty)] + U_\infty \quad (12a)$$

$$v(t) = \exp(-R_H t/H) [\cos(ft)(V_o - V_\infty) - \sin(ft)(U_o - U_\infty)] + V_\infty \quad (12b)$$

where  $R_H$  = drag velocity at the depth  $H$  (0.001 m/s),  $H$  = depth of wind driven flow (average study area depth),  $f$  = earth rotation rate (rad/s),  $U_o, V_o$  = velocity components at simulation start ( $t = 0$ ),  $U_\infty, V_\infty$  = asymptotic velocity components at  $t = \infty$ .

#### 4 OIL FATE CONCEPTS AND ALGORITHMS

Offshore, beyond the surf zone, COZOIL employs numerical concepts for oil spill fates simulation developed previously (Mackay *et al.*, 1980; Reed, 1980; Payne *et al.*, 1984; Spaulding *et al.*, 1986). Inside the surf zone, many additional concepts have been incorporated, in some cases without strong empirical evidence for values of the necessary parameters. In such cases, the user is given optional control over parametric values.

##### 4.1 Spreading

Spreading of a surface slick offshore is computed according to the gravity-viscous formulation of Fay (1971) and Hoult (1972) as modified by Mackay *et al.* (1980). The rate of change of surface area,  $A$  ( $m^2$ ), with time,  $t$  (s) is:

$$dA/dt = K_1 A^{0.33} (V/A)^{1.33} \quad (13)$$

Here  $V$  is slick volume ( $m^3$ ) and the constant  $K_1$  is set to 150/s (Mackay *et al.*, 1980).

Spreading of surface slicks in the surf zone is limited to the longshore direction. Transverse to the shoreline, compression of the slick occurs due to wind and wave/current forces on the slick and impedance to forward motion by the shoreline. (If the wind is offshore, the slick will be transported away from the coast, and the following discussion does not apply.)

Attempts were made to incorporate the work of Buist & Twardus (1984) and Buist (1987), who present data for the equilibrium thickness of small (< 1 kg) oil slicks spreading against wind in a wind tunnel. Their definition of the equilibrium thickness is that thickness at which the spreading and wind forces balance. At this point, the acceleration of the slick edge is zero, but the velocity in general is non-zero. Investigation of the dynamic behavior of the equation for one-dimensional spreading used by Buist & Twardus (1984) indicates that the location of the slick edge

oscillates in time, such that the equilibrium thickness occurs when the velocity of the slick edge is a maximum (i.e. when the acceleration is zero and the thickness itself is changing most rapidly). Unfortunately, their analysis is therefore not useful for the COZOIL model in which winds are in general unsteady, and coastal slicks are constantly changing mass and shape.

In view of the above, certain simplifying assumptions were used in formulating slick spreading in the surf zone. These are:

- (1) oil slick thickness is uniform
- (2) tendency of a slick to spread remains a function of area and thickness, as offshore
- (3) tendency to compress is proportional to the onshore wind stress on the slick
- (4) circulation of oil within the slick is negligible

Little error is introduced as a result of assumption (1) relative to the thick slick/thin slick conceptualization since over 90% of the mass is associated with the thick slick (Mackay *et al.*, 1980). Assumption (2) simply reflects the parameterization of the spreading process (equation (13)), wherein the mean effects of chemical composition and environmental processes are represented by a single rate parameter.

For an infinitesimal element of oil (Fig. 5), we assume that the spreading force in the onshore-offshore direction is balanced by the wind stress. In the alongshore direction, spreading occurs as usual. From equation (13), the rate of change of the radius due to the spreading force is:

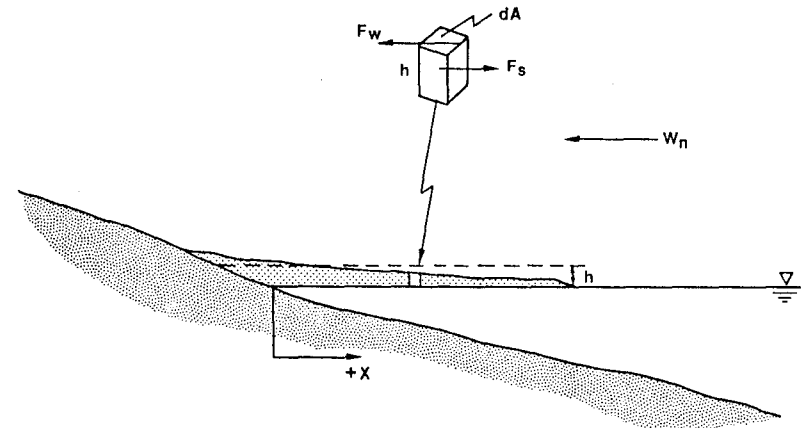


Fig. 5. Schematic oil slick driven against the shore by wind. Spreading/contracting is modelled as the resultant of the wind force  $F_w$  and the spreading force  $F_s$ .

$$dR/dt = 0.5K_A \delta^{4/3} \pi^{-2/3} R^{1/3} \quad (14)$$

where  $\delta$  is the mean slick thickness and  $R$  is mean slick radius. If the volume of the slick is constant (i.e. we neglect evaporation, entrainment, and emulsification during a computational timestep), then the rate of change of the thickness  $\delta$  in terms of the radius  $R$  is:

$$d\delta/dt = -2\delta/R \cdot dR/dt \quad (15)$$

and the acceleration of the slick edge, due to spreading forces only, still is:

$$d^2R/dt^2 = -1.5K_A \delta^{4/3} \pi^{-2/3} R^{-1/3} dR/dt \quad (16)$$

Here we see that the spreading force opposes the spreading velocity. The wind stress due to a wind speed  $W_N$  over an element of our ideal slick of uniform thickness is then:

$$\tau = \rho_a C_D W_N^2 dA \quad (17)$$

in which  $\rho_a$  = density of air (kg/liter),  $C_D$  = stress coefficient,  $dA$  = area element ( $m^2$ ),  $W_N$  = wind speed normal to and directed towards the coast (m/s).

The spreading force plus the wind stress force (Fig. 5) give the net acceleration of the element:

$$\rho_{oil} h dA d^2R/dt^2 - \rho_{air} C_D W_N^2 dA = \rho_{oil} h dA d^2R_T/dt^2 \quad (18)$$

where we have used  $R$  to denote radial changes due to spreading alone, as before, and  $R_T$  for the net radial change. Then:

$$d^2R_T/dt^2 = d^2R/dt^2 - \rho_{air} C_D W_N^2 / \rho_{oil} h \quad (19)$$

Slicks in contact with the coastline become elliptical with the major axis alongshore, and the spreading velocity of the major radius given by (13). The dynamics of the minor radius of the slick, oriented transverse to the shoreline, are then governed by (19).

#### 4.2 Evaporation

Evaporation of hydrocarbons from a surface slick is computed using the methods of Payne *et al.* (1984). The parent oil is represented by a series of constituents differentiated by boiling point, density, and molecular weight. The mass transfer rate from the slick for the  $i$ th constituent is:

$$dm_i/dt = K_2 P_i A f_i M_i / RT \quad (20)$$

where  $P_i$  = vapor pressure (atm) of  $i$ th constituent,  $A$  = slick area ( $m^2$ ),

$f_i$  = fraction of remaining slick consisting of constituent  $i$ ,  $M_i$  = molecular weight (g/mol) of constituent  $i$ ,  $R$  = gas constant ( $8.206 \times 10^{-5}$  atm  $- m^3$ /mol  $- K$ ),  $T$  = temperature (K).

The mass transfer coefficient  $K_2$  is that of Mackay & Matsugu (1973):

$$K_2 = 0.029 W^{0.78} D^{-0.11} S_c^{-0.67} \sqrt{(M_i + 29)/M_i} \quad (21)$$

where  $W$  = wind speed (m/h),  $D$  = slick diameter (m).

Following Mackay *et al.* (1980), we use a Schmidt number  $S_c$  for cumene, 2.7. The molecular weight term in equation (21) is a correction for diffusion in air (Payne *et al.*, 1984).

Evaporation on the foreshore follows the same computational procedures as on the water surface. Surface oil entering coastal lagoons or deposited on the backshore evaporates at the mean rate for oil on the beach during each timestep. This approximate procedure conserves both computer storage and processing time, while retaining a realistic evaporation rate governed by the composition of the oil spilled.

#### 4.3 Entrainment/dissolution

Entrainment and dissolution represent the only pathways for removal of mass from a surface slick other than evaporation. Unlike evaporation, entrainment is assumed to occur equally across all boiling point constituents of the oil. Dissolution is not modelled explicitly as a process separate from entrainment.

The user has two options for oil-entrainment algorithms. The first is that proposed by Audunson (1979) and modified by Spaulding *et al.* (1982); the mass transfer rate (per day) is:

$$dm/dt = 0.4mW^2 e^{-0.5t/W_o^2} \quad (22)$$

where  $m$  = mass of spilllet (mt),  $W$  = wind speed (m/s),  $t$  = time (days) since spilllet release,  $W_o$  = reference wind speed (8.5 m/s).

The second alternative algorithm is that proposed by Mackay *et al.* (1980), which gives a mass transfer rate (per hour) of:

$$dm/dt = 0.11m(1+W)^2/(1+50\mu^{0.5}\delta\sigma) \quad (23)$$

where  $\mu$  = dynamic viscosity (cp),  $\delta$  = slick thickness (cm),  $\sigma$  = oil-water interfacial tension (dyne/cm).

Entrainment of oil from a surface slick inside the surf zone is computed using the same algorithm as was specified by the user outside the surf zone. An entrainment procedure based explicitly on wave spectrum

characteristics (e.g. Spaulding *et al.*, 1982) would allow for future inclusion of increased surf zone turbulence.

#### 4.4 Emulsification

The viscosity  $\mu$  (cp) is allowed to increase for petroleum products according to a 'mousse formation' algorithm, also from Mackay *et al.* (1980). The rate of incorporation of water into the slick is:

$$dF_{wc}/dt = 2 \times 10^{-6} (W + 1)^2 (1 - F_{wc}/C_3) \quad (24)$$

where  $F_{wc}$  = fraction of water in oil,  $W$  = wind speed (m/s),  $C_3 = 0.7$  for crude oils and heavy fuel oils (Mackay *et al.*, 1982).

Gasoline, kerosene, and light diesel fuel are assumed not to form emulsions with water (Payne & Phillips, 1985). The resultant viscosity  $\mu$  of the oil in the slick is then computed using the Mooney (1951) equation:

$$\mu/\mu_o = \exp(2.5F_{wc}/(1.0 - 0.65F_{wc})) \quad (25)$$

in which  $\mu_o$  is the viscosity of the parent oil.

The effect of evaporation on viscosity is modeled as:

$$\mu = \mu_o \exp(C_4 F_{evap}) \quad (26)$$

where  $F_{evap}$  is the fraction evaporated from the slick.  $C_4$  varies in value between about 1 and 10 (Mackay *et al.*, 1982). The model uses  $C_4 = 1$  for gasoline, kerosene, and light diesel fuel, and  $C_4 = 10$  for other petroleum products.

#### 4.5 Advection

Offshore oil at the water surface is transported by the instantaneous sum of currents at the slick centroid. An additional transport at the surface is included to reflect wind and wave effects. Thus the net instantaneous slick transport velocity  $V$  is

$$V = V_T + V_W + 0.03 W \quad (27)$$

The tidal and wind-driven velocity components,  $V_T$  and  $V_W$ , are bilinearly interpolated within the grid system.

Subsurface oil is represented offshore by discrete particles entrained from surface slicks. The initial location of a particle is at a random location under the source slick at a depth  $z$  given by:

$$z = 0.5(1 + R^*)H \quad (28)$$

where  $R^*$  = random variate [ $-1 \leq R^* \leq 1$ ],  $H$  = wave height.

Subsequent transport of the particle is by the superposition of interpolated horizontal velocities, plus random components in both the horizontal and the vertical. The random components are computed as

$$V_R = R^* \sqrt{6D/\Delta t} \quad (29)$$

The diffusivity  $D$  is selected from the pair ( $D_H, D_V$ ), depending on whether a horizontal or vertical random walk step is being computed. The values of  $D_H$  and  $D_V$  are taken as 10 and 0.001 m<sup>2</sup>/s, respectively (Okubo, 1971; Csanady, 1973).

The offshore subsurface transport of entrained dissolved oil is largely irrelevant to the ultimate fate of oil along the coastline. This facility has been included to give the eventual users of COZOIL a more complete simulation capability. A set of 'nearest-neighbor' and compression algorithms is used to compress the arrays as new particles are created due to entrainment from surface slicks.

Advection in the surf zone is assumed to be dominated by the wave-induced current in the water column, with wind effects superimposed for surface slicks. The model uses the radiation stress theory of Longuet-Higgins (1970) as modified empirically by CERC (1984). The longshore velocity  $V$  is given in terms of the breaker height  $H_b$ , the angle between breaker crest and shoreline  $\alpha_b$ , and the beach slope  $m$  as:

$$V = 20.7 m (gH_b)^{1/2} \sin 2\alpha_b \quad (30)$$

The direction of transport is given by the angle  $\alpha_b$  relative to the shoreline. A surf zone 'subcell', with a width equal to the then-current surf zone width, is associated with each coastal cell. A fraction  $F_i$  of the mass of oil,  $m_i$ , which is in surf zone cell  $i$ , is transported into an adjacent surf zone cell each timestep:

$$F_i = V_i \Delta L / \Delta t \quad (31)$$

in which  $V_i$  is the longshore-transport velocity for this coastal cell (eqn (30)),  $\Delta L$  is the longshore coastal cell dimension, and  $\Delta t$  is the timestep. Whether the transport is into the prior ( $i - 1$ ) or the subsequent ( $i + 1$ ) surf zone cell depends on the incident wave angle  $\alpha_b$ .

#### 4.6 Deposition on foreshore surface

An oil slick which has contacted the shoreline may deposit oil on the foreshore if the water level does not exceed the foreshore height associated with that reach. First the model checks to determine that an empirical 'maximum holding thickness' (CSE & ASA, 1986; Gundlach,

1987) has not been exceeded. This limits the amount of oil able to be contained on any one beach segment, varying with beach type. When the tide is falling, the ratio of the newly exposed beach face to the onshore-offshore radius of the slick determines the fraction of the slick which is deposited.

Oil deposited on a previously clean foreshore carries with it the characteristics of the parent slick: viscosity, density and boiling point constituents. As additional oil comes ashore at the same location, perhaps from the same or another spill, the oil on the foreshore surface takes on the weighted average values of the above characteristics. This assumes complete mixing and is consistent with assumptions made elsewhere in the model.

#### 4.7 Deposition on backshore

If the water height exceeds the foreshore height, then a slick in contact with the shoreline will deposit oil on the backshore. As on the foreshore, the fraction of the slick which is deposited is determined by the ratio of newly exposed backshore to slick width.

#### 4.8 Entry into sediment/groundwater system

Observational evidence from several major oil spills, particularly the *Arrow* spill in Canada and the *Amoco Cadiz* in France, indicates that oil in association with the ground- or interstitial water within beaches may persist for several years (Vandermeulen & Gordon, 1976). The processes governing oil incorporation and movement within beach sediments and groundwater are not fully understood. However, by utilizing a series of formulations originally developed to predict fluid transport through land-based groundwater systems, it is possible to develop a computer-simulation model depicting penetration into beaches, and the subsequent removal or flushing of oil from this system.

Emery & Foster (1948) first described water-table movement in relation to tidal level. They found that the zone of water movement in the beach is essentially triangular with a bottom extending to a nodal or pivot point within the beach where there is little to no movement due to the tides (Fig. 6). They also noted that after the tidally-induced drainage of the beach, approximately 10% of the bulk volume still retained water.

In studying the groundwater characteristics in a New England sandy beach, Pollock & Hummon (1971) measured the degree of de-watering of the beach extending from near mean low water to the upper beach and found that the primary loss of groundwater occurred in the upper and

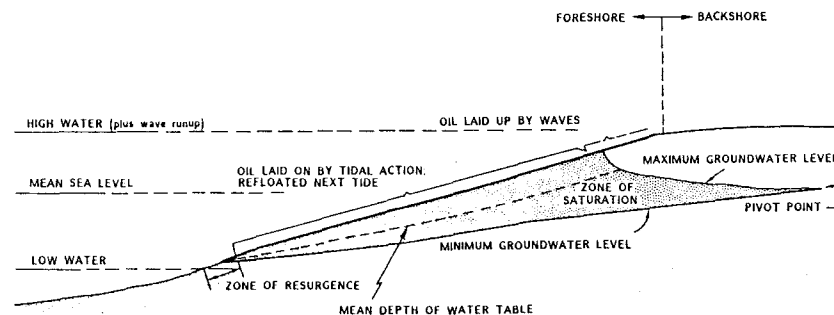


Fig. 6. Schematic of beach groundwater system.

interior portions of the beach (Fig. 6). Losses along the lower (seaward) edge of the beach are much less, since they are continually replenished from interior water. The input of additional water, as through rain or upland sources, would alter these conditions.

The movement of oil within beaches, or within or on the surface of beach groundwater, has not been studied in great detail. Vandermeulen & Gordon (1976) reported observations of oil associated with groundwater resulting from the *Arrow* oil spill in Nova Scotia. An estimate of the general level of oil released from the sediments was presented, indicating runoff losses in the parts-per-billion range.

The flow of oil from the surface of the foreshore into the sediments of the beach is a complex problem in three phase flow. If we neglect the fact that water draining from the beach may be replaced by air, the problem is reduced to a two phase, oil-water flow.

Three different regimes of fluid saturation can be distinguished (Convery, 1979). At very low saturations, water (the 'wetting-fluid') exists as pendular rings around grain contacts within the porous medium. These rings of fluid are completely isolated from one another, except perhaps for a thin film of water (phase) that coats the grain surface. This film, present at extremely low saturations, occurs on surface adsorption sites on the sediments. The film has a monomolecular thickness and may be continuous or discontinuous. Hydraulic pressures cannot be transmitted through the wetting-fluid in the pendular regime since it is not continuous.

If the saturation of water increases, the pendular rings expand and coalesce so that flow of the wetting phase is possible. Coincident with this development is a decrease in the saturation of the non-wetting phase. This saturation regime is labeled funicular. The phase distribution and flow behavior of fluids in the funicular regime are complex, and are

strongly a function of the saturation history of the porous medium.

With increasing saturation of the wetting phase, the non-wetting phase (oil) eventually becomes discontinuous. Commonly, droplets of the non-wetting phase become isolated in the larger pores of the medium. The non-wetting phase is in a condition of insular saturation. Non-wetting phase droplets become mobile only if a pressure discontinuity exists across them within the wetting phase to force them through capillary restrictions. Otherwise, the droplets are immobile and remain trapped within the pores. The insular drops will impede flow of the wetting phase to some extent.

In our analysis, we identify two regimes, the pendular and the insular, occurring at the foreshore surface in the presence of oil and in the zone of saturation (Fig. 6), respectively. Thus we neglect some complexities such as pore blockage by oil in the funicular regime, allowing the characteristics of the oil to control flow computations at the foreshore surface, and water to control flow within the beach.

In the COZOIL model, it is assumed that oil deposited on the beach foreshore may enter the sediment/groundwater system in two ways, the first by direct penetration, and the second by transport in wave overwash. The former process is simulated using standard fluid-sediment flow algorithms. The second process assumes that waves breaking and overwashing oil on the foreshore will carry with them dissolved and particulate ('water-accommodated') oil. This water-accommodated oil is assumed to travel into the sediments with, and at the same rate as, the water itself. Once within the groundwater system, the transport of oil is assumed to be governed by flushing of the groundwater and equilibrium partitioning kinetics between the adsorbed and water accommodated phases.

#### 4.9 Direct penetration of oil into sediments

The flow of oil from a surface deposit into the underlying sediments can be approximated by Darcy's law:

$$v = kg\rho(dh/dl)/\mu \quad (32)$$

where  $v$  = flow velocity (m/s),  $k$  = intrinsic permeability of the sediment ( $m^2$ ),  $g$  = gravitational acceleration ( $m/s^2$ ),  $\rho$  = fluid density ( $kg/m^3$ ),  $\mu$  = dynamic viscosity ( $N\cdot s/m^2$ ),  $dh/dl$  = pressure-head gradient (m/m).

The intrinsic permeability is computed with an equation from Krumbein & Monk (1943):

$$k = 7.6 \times 10^{-10} (MG)^2 e^{-1.31\phi} \quad (33)$$

in which  $MG$  = mean grain size (mm),  $\phi$  = inclusive graphic standard deviation ( $\phi$  units).

The depth of penetration during a timestep  $\Delta t$  is then, to first order,  $v\Delta t$ . The mass flux  $Q$  is

$$Q = A\rho v\Delta t \quad (34)$$

Here  $A$  is the surface area covered with oil. The maximum amount of oil which can enter the surface sediments is controlled by the net sediment porosity, corrected for any oil which has previously entered and remains in the foreshore surface sediment.

#### 4.10 Removal of surface oil by wave overwash

Observations by Owens *et al.* (1983, 1987) reflect the fact that wave exposure is an important parameter for the rate of removal of oil from the beach surface. An expression is therefore required for the rate at which oil is removed from the parent slick on the foreshore, and carried into the underlying sediments or returned to the active surf zone by wave action. Based on an empirical relationship (Thibodeaux, 1977, 1979), the mass transfer coefficient for relatively insoluble substances can be approximated by

$$h = 0.036(\rho V_b L/\mu)^{0.8}(\mu/\rho D_o)^{0.33} D_o/L \quad (35)$$

Equation (35) is an empirical relationship developed for relatively low Reynolds number flows on river bottoms. Surf zone Reynolds numbers are considerably higher. The rate given by Eqn (35) is therefore reduced by a factor of 0.01 in COZOIL, to better match observed rates (CSE & ASA, 1986; Gundlach, 1987).

The actual mass removal rate is then:

$$dm/dt = \rho h A \quad (36)$$

The mass removed from the oil on the foreshore surface by wave overwash is not all carried into the groundwater. Some fraction is carried back into the surf zone with the retreating wave. This oil in the surf zone is then further partitioned between the water column and the water surface, depending on the size range of the oil particles relative to the surf zone turbulence.

#### 4.11 Removal from the sediment/groundwater system

Oil in the beach groundwater system probably exists in three phases, as described above. In the pendular phase, oil is the primary fluid within the sediment pores and may preclude penetration of water. If the oil in this phase has a relatively low viscosity, it may actually ride up and down

on the rising and falling water-table, as hypothesized by McLaren (1985) for diesel fuel in a gravel-sand beach. The second phase is droplets, which may adhere to sediment particles or become trapped within sediment pores. The third is a dissolved phase, whose transport is governed by movement of the groundwater itself.

Oil which has penetrated the surface sediments via equation (34) and remains above the mean water-table (Fig. 6) may be removed to the surf zone if the beach is subject to erosion by the present wave field. A basic assumption here is that the presence of the oil will not appreciably alter erodibility of the beach sediments. Following Sunamura & Horikawa (1974), COZOIL incorporates a dimensionless erosion/accretion parameter  $G_0$ :

$$G_0 = (H_0/L_0)(\tan\beta)^{0.27}/(D_{50}/L_0)^{0.67} \quad (37)$$

where  $H_0$  = deep-water wave height (m),  $L_0$  = deep-water wave length (m),  $\beta$  = offshore bottom slope,  $D_{50}$  = size of 50th percentile of sediment sample (m).

Beach erosion is assumed to occur for  $G_0 > 18$ , accretion for  $G_0 < 4$ , and equilibrium in between.

Observations of oil behavior within the beach groundwater system have shown that both low- and high-viscosity petroleum can enter the groundwater system in significant quantities and remain detectable for years afterwards (Vandermeulen & Gordon, 1976; Harper *et al.*, 1985; McLaren, 1985). Subsequent release of oil from groundwater appears to occur primarily at low tide (McLaren, 1985). The COZOIL model incorporates a relatively simple representation of oil in the beach groundwater system, a representation which nonetheless reproduces the observed behavior relatively well. The oil is partitioned between two phases, one of which is trapped by the sediments (an 'adsorbed' phase), and one which is transported with the groundwater (a 'water-accommodated' phase). We assume the equivalent to an equilibrium partitioning between oil in the adsorbed and water-accommodated phases (e.g. Thibodeaux, 1979),

$$C_a/C_{wa} = K_p C_{ss} F_c \quad (38)$$

in which  $C_a$  and  $C_{wa}$  are the concentrations of oil in the groundwater which are adsorbed and water accommodated, respectively.  $K_p$  is the partition coefficient,  $C_{ss}$  is the sediment concentration, and  $F_c$  is the fraction of the sediment which is composed of organic matter. From the fact that  $C_a + C_{wa} = C_T$ , the total concentration, equation (38) can be rewritten as:

$$C_{wa} = C_T / (1 + K_p C_{ss} F_c) \quad (39)$$

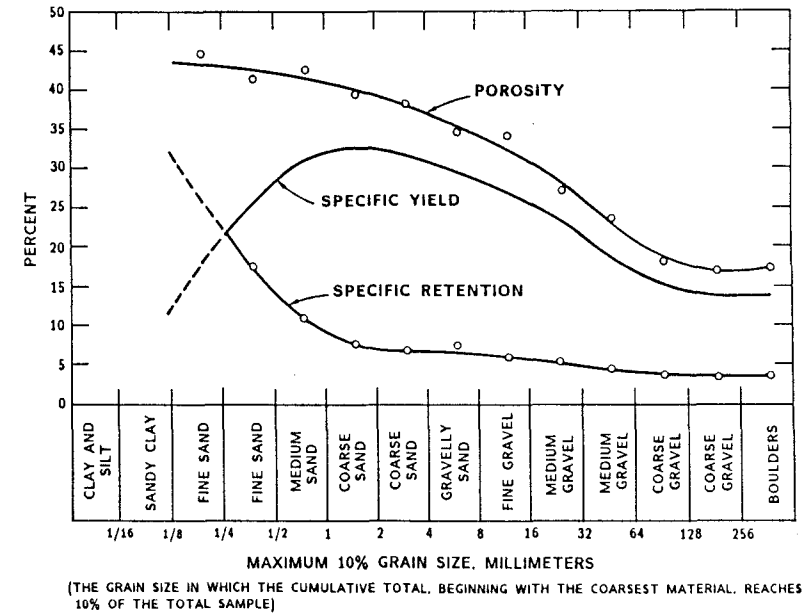


Fig. 7. Porosity, specific yield, and specific retention variations for various grain sizes (from Todd, 1959).

The mass removed per tidal cycle is then:

$$F_{wa} = S_y C_{wa} M / C_T \quad (40)$$

in which  $S_y$  is the specific yield of the sediment (Fig. 7), and  $M$  is the total mass of oil in the groundwater system of the beach.

#### 4.12 Reflotation

Oil on the beach face (foreshore surface) which has not penetrated the sediments may be refloat on a rising tide. As oil is refloat from the foreshore surface, it is combined with an existing spillet if one is present at that coastal location. In this case, the characteristics of the spillet become the mass-weighted characteristics of the spillet plus the newly refloat oil. If a spillet does not exist at the coastal cell where refloatation is occurring, a new spillet is formed.

#### 4.13 De-watering (de-emulsification)

Water which has become incorporated into oil during the process of emulsification may be released from oil-water mousse deposited on the

beach face. The rate of release, or de-emulsification, is dependent on the stability of the mousse. Stability is in turn a function of several factors (Payne & Phillips, 1985). Natural emulsifying agents such as asphaltene, waxes, and porphyrin complexes must be present. Viscosity also is important since higher viscosities tend to hinder movement of water within the mousse. Specific gravity, water content, and age of the emulsion may also contribute to stability. Detailed investigations by Berridge *et al.* (1968*a, b*) evaluated mousse formation and stability for several crude oils and five petroleum products. In general, the crude oils investigated formed relatively stable emulsions, whereas the refined products (e.g. diesel, kerosene, gasoline) did not form emulsions at all. The set of characteristics governing emulsion stability, however, appears to be sufficiently complex as to warrant a separate study. Here we assume a first order process for the loss of water from stranded mousse:

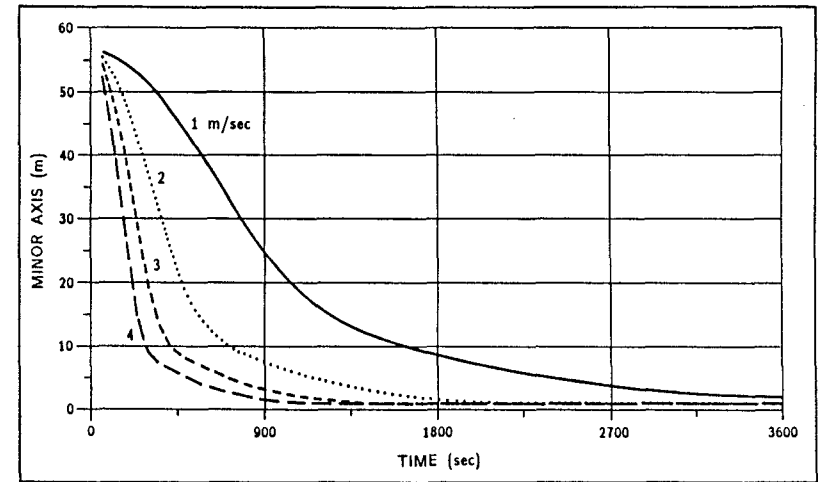
$$y = y_0 e^{-bt} \quad (41)$$

where  $y$  = fraction of water in oil at time  $t$ ,  $y_0$  = initial fraction of water in oil,  $b$  = constant.

## 5 SENSITIVITY STUDIES

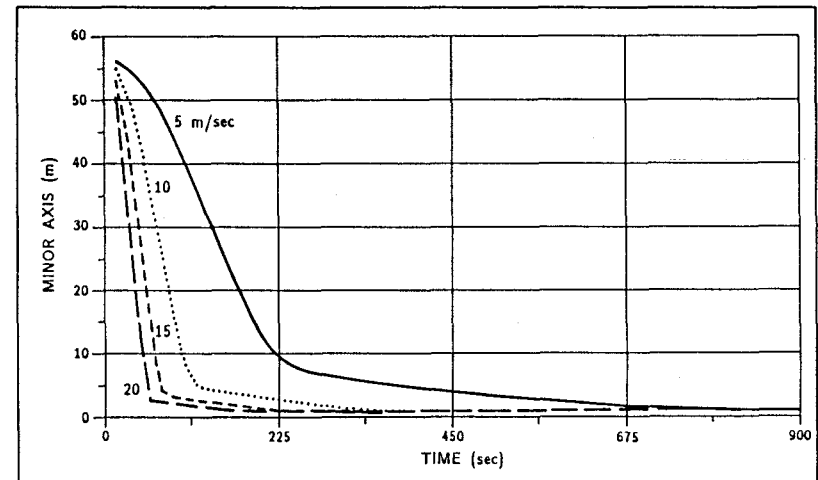
### 5.1 Spreading in the surf zone

The equation for spreading/compression of oil slicks in the surf zone balances wind stress normal to the shoreline against the gravity/viscous force to determine the rate of change of the onshore/offshore (minor) axis of the slick as a function of time. The longshore (major) axis increases according to the same rate equation used offshore. The dynamic behaviour of the minor axis of a  $100 \text{ m}^3$  oil slick under the influence of various onshore wind speeds is shown in Figs 8a and 8b. For these test cases, the slick was initiated with a thickness of 1 cm and a radius of about 56 m. A limiting minor axis length of 1 m was also specified. At a wind speed of 1 m/s, the time for the onshore/offshore axis to reach this limit is about 1 h, vs about 15 min at 4 m/s (Fig. 8a). At 15 m/s, the time to reach a 1-m minor axis length is about 4 min (Fig. 8b). It should be noted that these tests are independent of any other processes in the model. The surf zone wave field associated with 15 or 20 m/s winds, for example, would rapidly entrain surface oil into the water column, so that consideration of foreshortening rates at these higher wind speeds becomes moot.



(a)

Fig. 8a. Onshore-offshore foreshortening of a  $100 \text{ m}^3$  slick under the influence of 1, 2, and 4 m/s winds.



(b)

Fig. 8b. Onshore-offshore foreshortening of a  $100 \text{ m}^3$  slick under the influence of 5, 10, 15 and 20 m/s onshore winds.

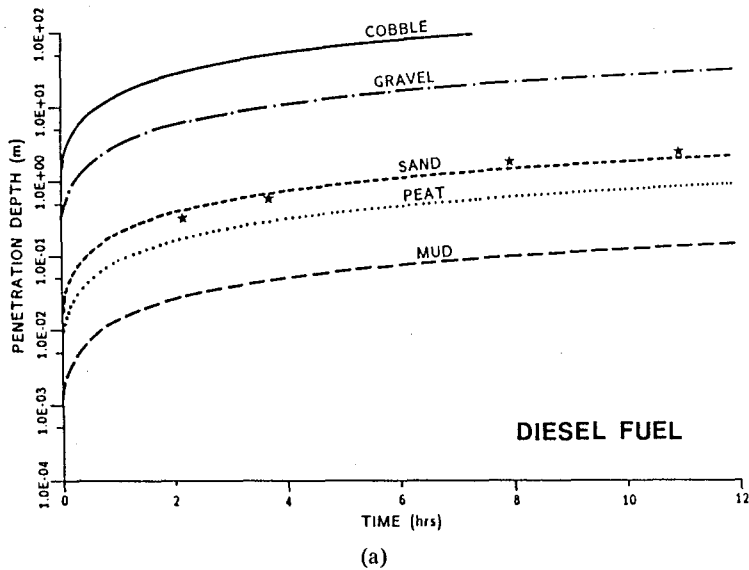


Fig. 9a. Penetration depth as a function of time for diesel fuel (viscosity = 11 cp) on various sediment types. Asterisks show data from laboratory tests by Holoboff & Foster (1987).

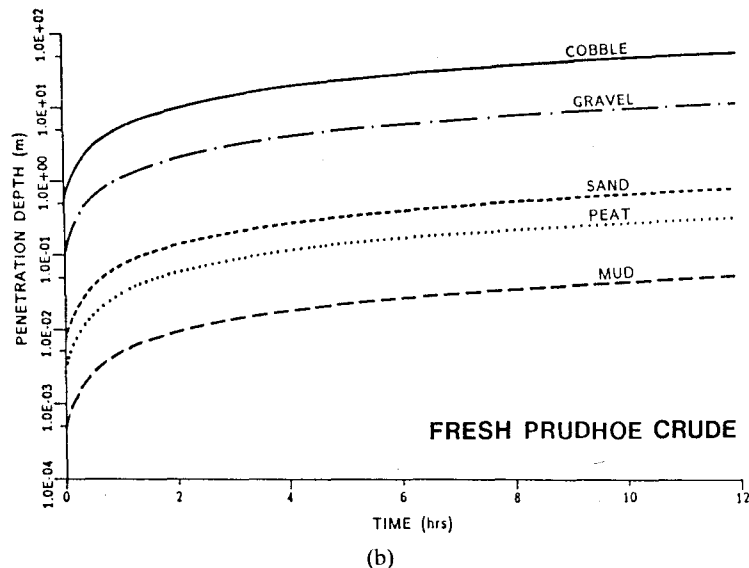


Fig. 9b. Penetration depth as a function of time for fresh Prudhoe Bay crude oil (viscosity = 35 cp) on various sediment types.

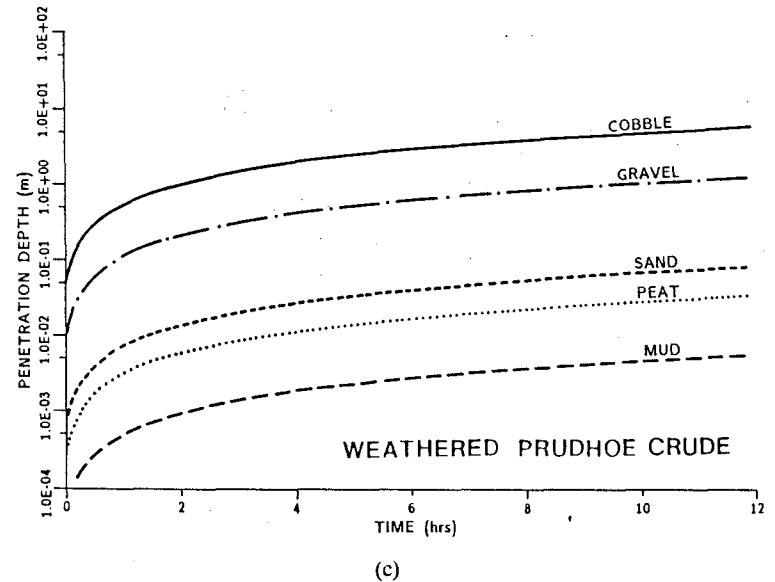


Fig. 9c. Penetration depth as a function of time for weathered Prudhoe Bay crude oil (viscosity = 350 cp) on various sediment types.

## 5.2 Penetration rates

Model tests were performed to demonstrate penetration rates as a function of sediment type and oil viscosity. In this case, the penetration equations are solved for an infinite sediment neglecting the presence of groundwater which is accounted for in the model. Figure 9a shows penetration depth as a function of time for a light diesel fuel in five sediment types. For comparison, data from a laboratory test of an equivalent viscosity oil in Canadian borrow pit sands (Holoboff & Foster, 1987) is shown. The calculated penetration rate for sand matches the observations quite well. The rates for other sediments are qualitatively as expected relative to the rate for sand.

Figure 9b shows penetration depths vs time for Prudhoe Bay crude, with a viscosity about three times that of light diesel. After 12 h, the Prudhoe Bay crude has penetrated to a depth of 1 m, vs about 3 m for the light diesel of Fig. 9a. Weathered Prudhoe Bay crude, with a viscosity of 350 cp, 10 times the viscosity of the fresh crude, reaches a depth of about 0.1 m after 12 h (Fig. 9c). These proportionalities are consistent with the fact that the penetration rate is inversely proportional to the viscosity.

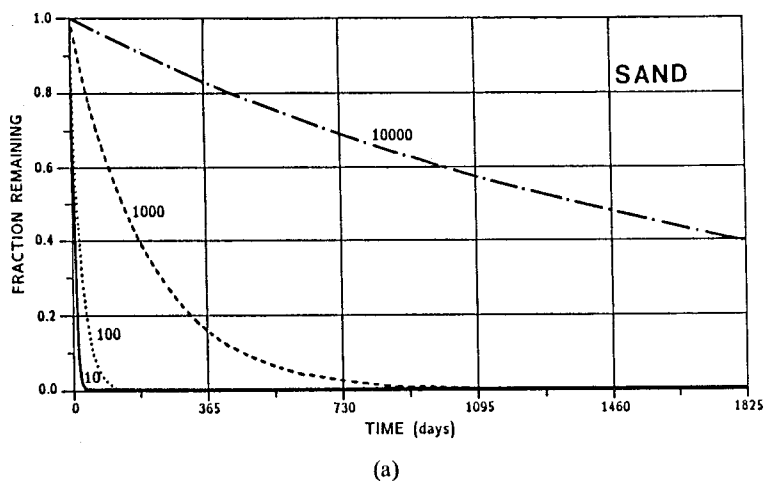


Fig. 10a. Retention of oil in a sand beach for various values of the partition coefficient  $K_p$ .

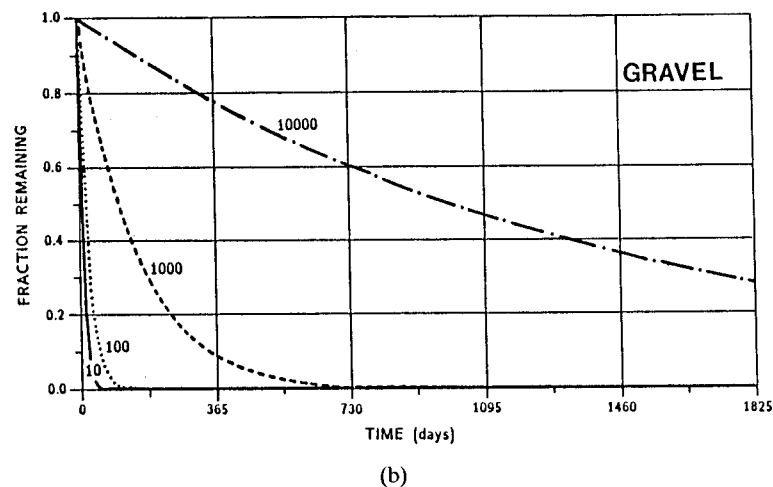


Fig. 10b. Retention of oil in a gravel beach for various values of the partition coefficient  $K_p$ .

### 5.3 Retention of oil in groundwater system

The retention of petroleum in the beach groundwater system is governed by equations (38)–(40). The partitioning coefficient,  $K_p$ , is an unknown parameter in this formulation. A series of simulations was therefore performed (Figs 10a–10d) to allow selection of an appropriate value for

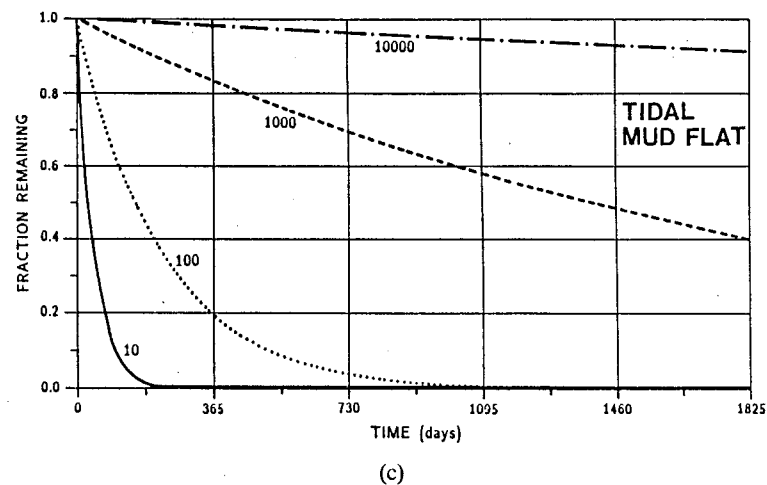


Fig. 10c. Retention of oil in a mud tidal flat for various values of the partition coefficient  $K_p$ .

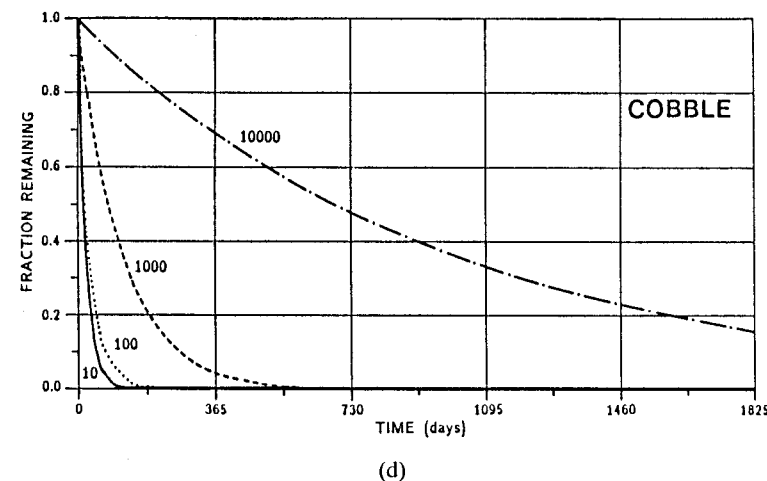


Fig. 10d. Retention of oil in a cobble beach for various values of the partition coefficient  $K_p$ .

$K_p$ . We estimate that a half-life for oil in a sandy or gravel beach is commonly about 6 months, and about 3 years in a mudflat. From Figs 10a–10d, we therefore have adopted a value for  $K_p$  of 1000 which the user has the option to adjust. The governing partitioning equation (38) shows that the removal rate will be equally sensitive to the fraction of the beach sediment which is composed of organic matter. The coefficients  $F_c$  for

various beach types are taken from Trask (1939), but again the user has the option to alter these default values.

A series of model test runs was performed to demonstrate overall model behavior for various types of coastal reaches. In each case, a single uniform straight stretch of coastline 5 km in length is simulated. One thousand barrels (141 mt) of Prudhoe Bay crude oil is released in 24 spilletts over 48 h. The release point is 1 km offshore and about midway along the reach. The wind is constant at 5 m/s, and is 10° away from being directly onshore. Only the reach type is changed from one test to the next.

The mass balance as a function of time for oil coming ashore on a sand beach is shown in Figs 11a–11d. Since the travel time from the oil release point 1 km offshore is about 2 h, the release of spilletts offshore is approximately balanced by spilletts arriving onshore, so that the oil mass on the water surface reaches an approximate steady state after the first 12 h (Fig. 11a). This oil is compressed against the shoreline by the wind, which reduces surface area and slows evaporation rates. Oil deposited on the shore does not spread further and is absorbed into the beach face. These factors combine to reduce the net amount of mass which will evaporate relative to the 20% expected for this oil in an offshore simulation. The tidal signal is clearly discernible in the trace of oil mass on the water surface (Fig. 11a) and shoreline surface (Fig. 11c), the rising tide corresponding to the increase in oil mass on the water surface and a decrease on the beach.

The longshore currents for this test are about 6 cm/s due to waves, plus 2 cm/s at the surface due to wind. The travel time from the reach midpoint to the boundary, 2.5 km, is therefore about 9 h for oil at the surface and 12 h for oil entrained in the surf zone water column. During the first 60 h of the simulation, surface oil leaving the model domain alongshore represents the primary contribution to oil which is 'outside' (Fig. 11a). In the longer term (e.g. 90 days, as shown in Fig. 11b), the lower level contribution from the surf zone becomes an additional important mechanism for oil removal from the study area. The transport of oil from the surf zone to the offshore water column and sea floor also becomes relatively important after the first 10 days (Fig. 11b).

Figure 11c shows a detailed mass balance for the oil on the shore. The top trace, 'Total Ashore', corresponds to the trace labeled 'Ashore' in Fig. 11a. As oil comes ashore, it rapidly penetrates the foreshore surface sediments, and thereafter begins to enter the beach groundwater system. The 'Foreshore Surface' trace in Fig. 11c is 180° out of phase with the oil on the water surface (Fig. 11a), since deposition on the beach surface is the opposite of refloating.

Figure 11d shows the same trace as Fig. 11c, but carried out for a period of 90 days. There is no erosion of the beach in this test case, so that the only pathway for oil in the foreshore surface sediments is into the groundwater system (Fig. 1). From the groundwater system, the oil is gradually flushed out into the surf zone, and then removed rapidly to the offshore water column (Fig. 11d).

The overall mass balance for a mudflat is shown in Fig. 12a. Here relatively little oil is initially retained in the sediments, but release is much slower than for sand. This difference is due not only to increased organic content, but also to relatively low specific yield of mud sediments during ebb tides. That oil which does penetrate these fine-grained sediments is therefore flushed out relatively slowly (Fig. 12b). The removal rate from a gravel beach (Figs 13a, 13b) is higher than that for sand, due to lower organic content and more rapid flushing.

In general, a COZOIL simulation will consist of multiple reaches of various lengths and types. In such cases, the model computes and retains complete, detailed mass balance information for each reach, as shown in Figs 11a–11d for the sandy beach.

## 6 CONCLUSIONS

The coastal zone oil spill model is a composite of concepts and algorithms drawn from a variety of disciplines. Some of these numerical representations are well established in the relevant literature, others are relatively new and hypothetical. Where established algorithms have been used as, for example, Darcy's Law, in the computation of oil penetration rates into beach sediments, tests of the code have been performed to insure that produced results are comparable with observations. Where new algorithms have been developed, or concepts have been applied in new ways, tests against empirical data are even more important. Unfortunately, such data have not always been available and future experimental work may be indicated in such cases.

COZOIL incorporates a modification to the radial spreading equation of Fay (1971) and Houtt (1972) as re-cast by Mackay *et al.* (1980). This modification allows a circular slick which contacts the shoreline to become elliptical, with the minor axis dynamics governed by a force balance between the onshore component of the wind stress and the spreading force. The rate of onshore-offshore foreshortening is proportional to a drag coefficient. As no data have been identified in the literature to establish foreshortening rate as a function of wind speed, the drag coefficient has been set equal to an established value for wind on

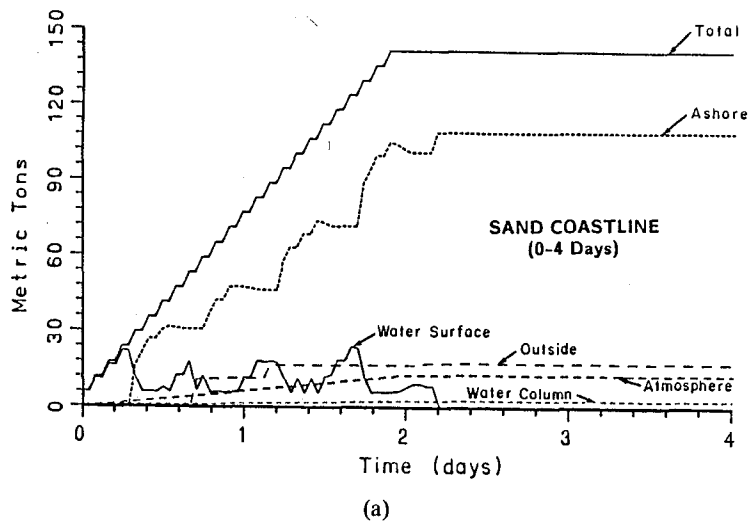


Fig. 11a. Overall mass balance for Prudhoe Bay crude oil coming ashore on a sand beach (first 4 days). 'Outside' refers to oil which has been transported out of the model boundaries.

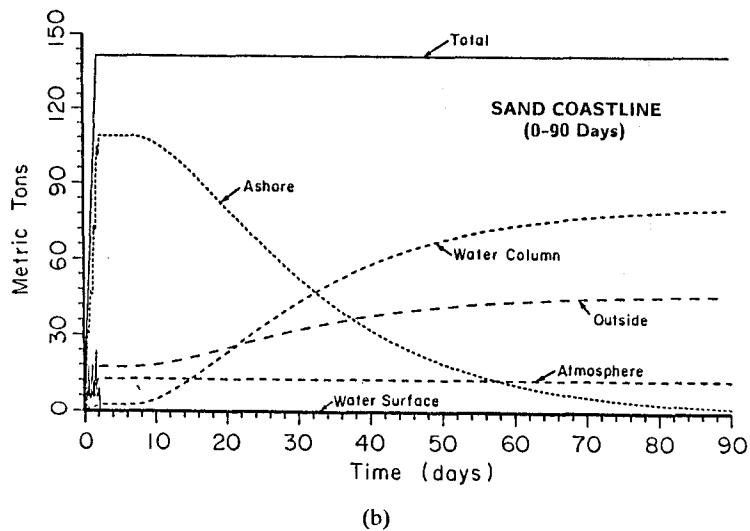


Fig. 11b. Overall mass balance for Prudhoe Bay crude oil coming ashore on a sand beach (first 90 days).

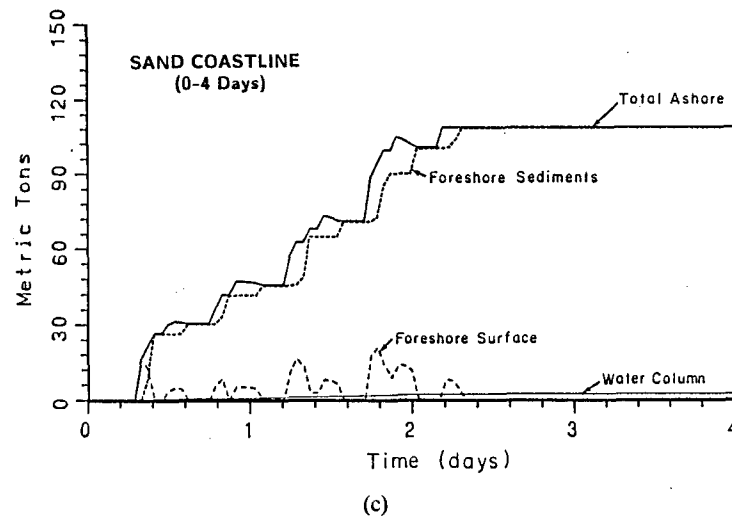


Fig. 11c. Mass balance for Prudhoe Bay crude oil on the sand coastline of Fig. 11a (first 4 days).

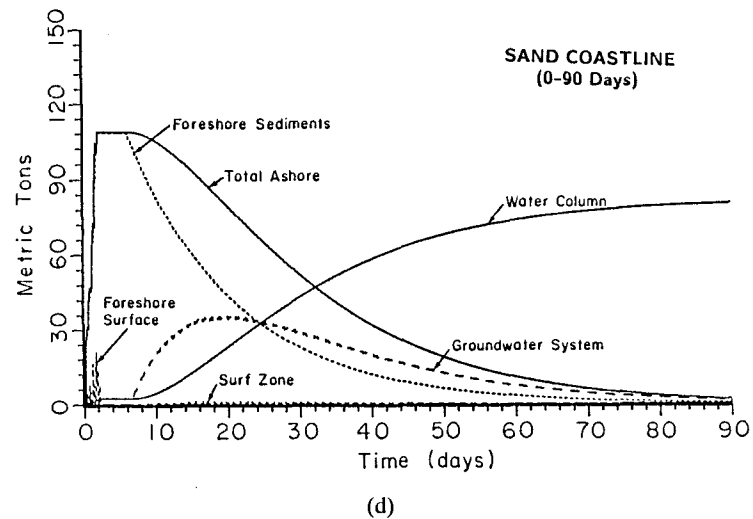
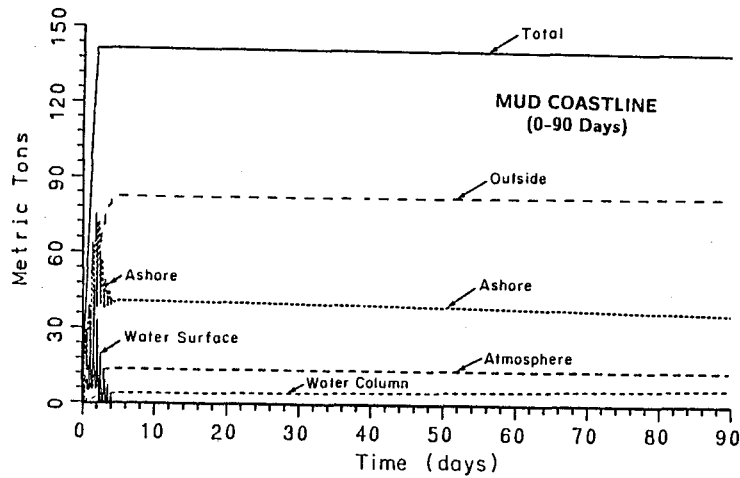
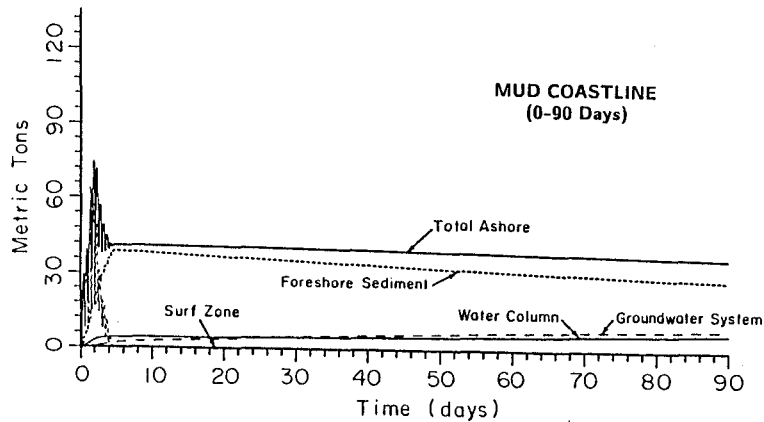


Fig. 11d. Mass balance for Prudhoe Bay crude oil on the sand coastline of Fig. 11a (first 9 days).



(a)

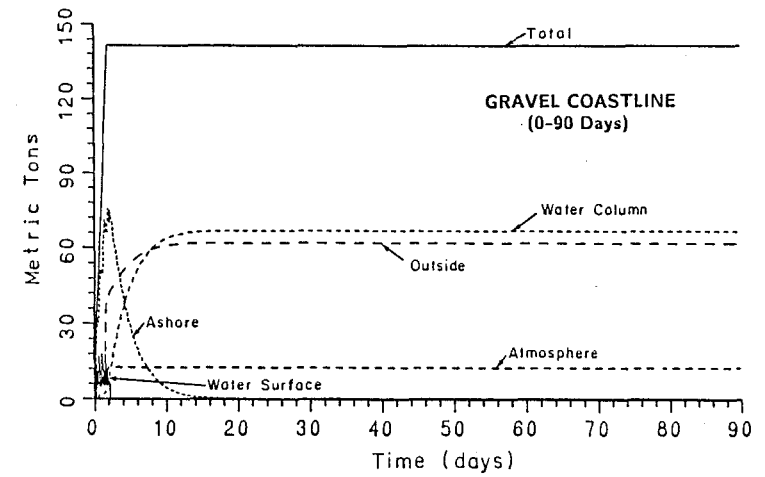
Fig. 12a. Overall mass balance for Prudhoe Bay crude oil coming ashore on a tidal mudflat.



(b)

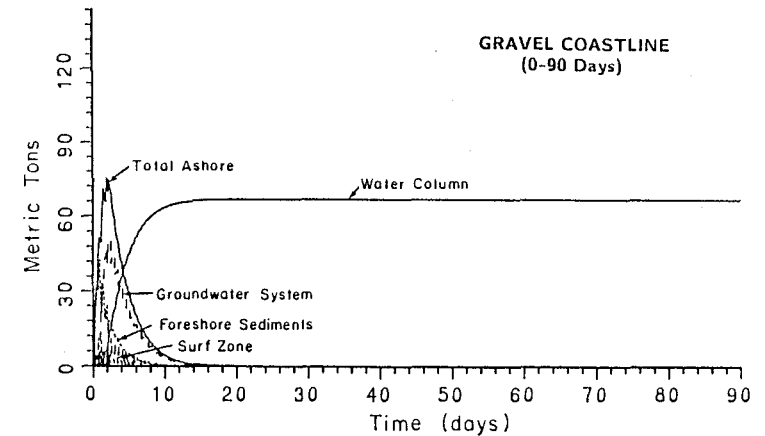
Fig. 12b. Mass balance for Prudhoe Bay crude oil on the mudflat of Fig. 12a.

water. The resulting behavior of the algorithms has been reported and appears reasonable, but empirical support would strengthen this aspect of the model. The onshore-offshore foreshortening and alongshore spreading of oil spilletts affects the evaporation rate through the surface area, the entrainment rate through the thickness, and the deposition



(a)

Fig. 13a. Overall mass balance for Prudhoe Bay crude oil coming ashore on a gravel beach.



(b)

Fig. 13b. Mass balance for Prudhoe Bay crude oil on the gravel beach of Fig. 13a.

rate on the coastline through both the longshore and transverse dimensions of the slick.

All of the algorithms for deposition of oil from a surface slick onto a shoreline are new to the field of oil spill modeling. Results of model tests

compare well with overall mass deposition estimates. It would be useful to plan and prepare a study to observe and record dynamic deposition rates through several tidal cycles during spills of opportunity. In cases for which coastal cleanup is not subsequently undertaken, studies of penetration rates, long-term retention rates, and detailed observations of oil behavior within the beach groundwater system would also strengthen the model.

It is clear from empirical field data that wave exposure is an important parameter in determining removal rates for oil on the foreshore surface. This fact is incorporated into the COZOIL model with an empirical mass transfer equation designed for less turbulent regimes than is typical in the marine surf zone. An adjustment in the proportionality constant was made to more accurately reproduce observations on removal rates which are available (CSE & ASA, 1986). As part of the previously suggested studies using spills of opportunity, some carefully quantified measures of removal rates as a function of beach and wave parameters would be useful.

#### ACKNOWLEDGMENTS

Primary support for this work was provided by the United States Department of Interior, Minerals Management Service, Alaska Regional Office. Dr William Benjey of the Minerals Management Service acted as technical contract monitor for the project. Some of this work was performed while the lead author held a Senior Scientist Fellowship with the Physical Oceanographic Group of the Oceanographic Center in Trondheim, now part of OCEANOR — Oceanographic Company of Norway A/S. The authors would like to thank Liz Kard, Kate Sexton, and Jan Hopp of Applied Science Associates and Anne-Kristin Sellevoll of Oceanor, for preparation of this manuscript.

#### REFERENCES

- Audunson, T. (1979). Fate of oil spills on the Norwegian continental shelf. Presented at 1979 Oil Spill Conf., API Publ. No. 4308. Washington, D.C.
- Berridge, S. A., Dean, R., Fallows, R. & Fish, A. (1968a). The properties of persistent oils at sea. In *Proc. Sympos. on Scientific Aspects of Pollution of the Sea by Oil*, ed. P. Heggle, pp. 2-11.
- Berridge, S. A., Thew, M. & Loriston-Clarke, A. (1968b). The formation and stability of emulsions of water in crude petroleum. *Journal of the Institute of Petroleum*, **54**, 333-57.
- Berkhoff, J. C. W. (1972). Computation of combined refraction-diffraction. *Proc. 13th Int. Conf. on Coastal Engineering*. American Society of Civil Engineers, Vol. 1, pp. 471-90.
- Berkhoff, J. C., Booy, N. & Radder, A. (1982). Verification of numerical wave propagation models for simple harmonic linear water waves. *Coastal Eng.*, **6**, 255-79.
- Buist, I. A. (1987). A preliminary feasibility study of in-situ burning of spreading oil slicks. *Proc. 1987 Oil Spill Conference*, API Publ. No. 4452, Amer. Petrol Inst., Wash, DC, pp. 359-67.
- Buist, I. A. & Twardus, E. M. (1984). In-situ burning of uncontained oil slicks. *Proc. Seventh Annual Arctic Marine Oil Spill Program*, Environ. Canada, Ottawa, pp. 127-54.
- CERC (1984). *Shore Protection Manual*, Vol. 1. US Army Corps of Engineers, Coastal Engineering Research Center, Ft. Belvoir, VA.
- Convery, M. P. (1979). The behavior and movement of petroleum products in unconsolidated surficial sediments. Report to National Wildlife Federation and American Petroleum Institute.
- Csanady, G. T. (1973). *Turbulent Diffusion in the Environment*. D. Reidel, Boston, MA.
- CSE & ASA (Coastal Science and Engineering, Inc. and Applied Science Associates, Inc.) (1986). Development of a coastal oil spill smear model. Phase I. Analysis of available and proposed models. Report to US Dept. Interior, MMS, Anchorage, Alaska. Contract 14-12-0001-30130.
- Dally, W. R., Dean, R. G. & Dalrymple, R. A. (1984). Modeling wave transformations in the surf zone. Miscellaneous Paper CERC-84-8, US Army Waterways Experiment Station, Vicksburg, MS.
- Ebersole, B. A., Cialone, M. A. & Prater, M. D. (1986). Regional coastal processes numerical modeling system Report 1. RCPWAVE — a linear wave propagation model for engineering use. Dept. of the Army, Wateredge Experiment Station, Vicksburg, MS.
- Emery, K. O. & Foster, J. F. (1948). Water table in marine beaches. *J. Marine Res.*, **7**, 644-54.
- Fay, J. A. (1971). Physical processes in the spread of oil on a water surface. In *Proc. 1971 Oil Spill Conf.*, American Petroleum Inst., Washington, DC, pp. 463-7.
- Ford, R. G. (1985). Oil slick sizes and length of coastline affected: a literature survey and statistical analysis. Final report to US Department of Interior, MMS Contract No. 14-12-0001-30226.
- Gundlach, E. R. (1987). Oil holding capacities and removal coefficients for different shoreline types to computer simulate spills in coastal waters. *Proc. 1987 Oil Spill Conference*, pp. 451-7.
- Harper, J. R., Musklin, G. A., Green, D., Hope, D. & Vandermeulen, J. (1985). Experiments on the fate of oil in low energy marine environments. In *Proc. Eighth AMOP Conf.*, Environment Canada, Ottawa, pp. 383-99.
- Holoboff, A. & Foster, R. (1987). Saturation/penetration of Norman wells crude oil into Ukalerk Borrow Pit sand. *Proc. Tenth Annual Arctic Marine Oil Spill Program*, Ottawa, Canada, pp. 63-78.
- Horikawa, K. & Kuo, C. (1966). A study of wave transformation inside the surf zone. *Proc. of 10th International Conf. on Coastal Eng.*, A.S.C.E., pp. 217-33.

- Hoult, D. P. (1972). Oil spreading on the sea. *Ann. Rev. Fluid Mech.*, pp. 341-68.
- Izumiya, T. (1984). A study of wave and wave-induced nearshore currents in the surf zone. PhD dissertation, University of Tokyo, Japan.
- Krumbein, W. C. & Monk, G. D. (1943). Permeability as a function of size parameters of unconsolidated sands. *Trans. Amer. Inst. Mech. Engng.*, **151**, 153-63.
- Longuet-Higgins, M. S. (1970). Longshore currents generated by obliquely incident sea waves. *Journal of Geophysical Research*, **75**, 6778-801.
- Mackay, D. & Matsugu, R. S. (1973). Evaporation rates of liquid hydrocarbon spills on land and water. *Can. J. Chem. Eng.*, **51**, 434-9.
- Mackay, D., Buist, I., Mascaraenas, R. & Paterson, S. (1980). Oil spill processes and models. Report EE-8, University of Toronto, Report to Environment Protection Service, Ottawa, Ontario, Canada.
- Mackay, D., Shiu, W. Y., Hossain, K., Stiver, W., McCurdy, D., Paterson, S. & Tebeau, P. (1982). Development and calibration of an oil spill behaviour model. US Coast Guard Research and Development Center, Contr. No. DTICG-39-81-C-80294, Rept No. CG-D-27-83.
- McLaren, P. (1985). Behaviour of diesel fuel on a high energy beach. *Mar. Poll. Bull.*, **16**, 191-6.
- Mooney, M. (1951). The viscosity of a concentrated suspension of spherical particles. *J. Colloidal Science*, **10**, 162-70.
- Okubo, A. (1971). Oceanic diffusion diagrams. *Deep Sea Research*, **8**, 789-802.
- Owens, E., Harper, J., Foget, C. & Robson, W. (1983). Shoreline experiments and the persistence of oil on arctic beaches. *Proc. 1983 Oil Spill Conference*. API Publ. No. 4336, Amer. Petrol. Inst., Washington, DC, pp. 261-8.
- Owens, E. H., Robson, W., Humphrey, B., Hope, D. & Harper, J. (1987). The fate of stranded oil four years after an experimental spill on sheltered gravel beach. *Proc. 1987 Oil Spill Conference*, pp. 473-8.
- Payne, J. R. & Phillips, C. R. (1985). *Petroleum Spills in the Marine Environment. The Chemistry and Formation of Water-in-Oil Emulsions and Tar Balls*. Lewis, Chelsea, MI.
- Payne, J. R., Kirstein, B. E., McNabb, G. D. *et al.* (1984). Multivariate analysis of petroleum weathering in the marine environment-subarctic. In Environmental Assessment of the Alaska Continental Shelf. Final Report of Principal Investigators, Vol. 22, US Dept. Commerce, NOAA/NOS/OAD. US Dept. Interior, MMS, Vol. II.
- Pollock, L. W. & Hummon, W. D. (1971). Cyclic change in interstitial water content, atmospheric exposure, and temperature in a marine beach. *Limnol. and Oceanogr.*, **16**, 522-35.
- Reed, M. (1980). An oil spill — fishery interactional model: development and applications. PhD Thesis, Dept. Ocean Engineering, University of Rhode Island.
- Seip, K. L., Brekke, K. A., Kveseth, K. & Ibrekk, H. (1986). Models for calculating oil spill damages to shores. *Oil and Chemical Pollution*, **3**, 69-81.
- Spaulding, M. L., Jayko, K. & Anderson, E. (1982). Hindcast of the Argo Merchant spill using the URI oil spill fates model. *J. Ocean Engineering*, **9**, 455-82.
- Spaulding, M. L., Isaji, T., Anderson, E., Turner, C., Jayko, K. & Reed, M. (1986). Oil spill trajectory and fates modeling for Shumagin Basin, Alaska. Report to NOAA/OCSEAP.

- Sunamura, T. & Horikawa, K. (1974). Two dimensional beach transformation due to waves. *Proc. 14th Coastal Engineering Conf.*, Copenhagen, Denmark, pp. 920-38.
- Thibodeaux, L. J. (1977). Mechanisms and idealized dissolution modes for high density immiscible chemicals spilled in flowing aqueous environments. *AI Che.*, **23**, 553-5.
- Thibodeaux, L. J. (1979). *Chemodynamics*. John Wiley and Sons, New York.
- Todd, D. K. (1959). *Ground Water Hydrology*. John Wiley & Sons, New York.
- Trask, P. D. (1939). *Organic Content of Recent Marine Sediments*. In *Recent Marine Sediments, A Symposium*, ed. P. D. Trask. Dover Publications, New York, pp. 428-53.
- Vandermeulen, J. H. & Gordon, J. H. Jr (1976). Reentry of 5-year-old stranded bunker C fuel oil from a low-energy beach into the water, sediments, and biota of Chedabucto Bay, Nova Scotia. *J. Fisheries Research Board, Canada*, **55**, 2002-10.
- Weggel, J. R. (1972). Maximum breaker height. *Journal of the Waterways, Harbors, and Coastal Engineering Division*, **78**, No. WW4, 529-48.